

Systematics of heavy-ion fusion hindrance at extreme sub-barrier energies

C. L. Jiang, B. B. Back, H. Esbensen, R. V. F. Janssens, and K. E. Rehm

Physics Division, Argonne National Laboratory, Argonne, IL 60439

(Dated: July 9, 2018)

The recent discovery of hindrance in heavy-ion induced fusion reactions at extreme sub-barrier energies represents a challenge for theoretical models. Previously, it has been shown that in medium-heavy systems, the onset of fusion hindrance depends strongly on the "stiffness" of the nuclei in the entrance channel. In this work, we explore its dependence on the total mass and the Q -value of the fusing systems and find that the fusion hindrance depends in a systematic way on the entrance channel properties over a wide range of systems.

PACS numbers: 24.10.Eq, 25.70.Jj

During the last thirty years of sub-barrier fusion studies, three important observations have been made: 1) the discovery of sub-barrier fusion enhancement associated with couplings to the intrinsic excitations of the participating nuclei [1, 2, 3, 4]; 2) measurements of the spin-distributions of the fused-compound nuclei and their theoretical description [5]; 3) the introduction of the concept of barrier distributions and their subsequent detailed measurements [6, 7]. In these studies it has been found that new representations of the fusion cross sections, such as the spin distribution $d\sigma(l)/dl$, the moments $\langle l \rangle$ and $\langle l^2 \rangle$ of this distribution, as well as the quantity $d^2(E\sigma)/dE^2$ associated with the distribution of fusion barriers [6], are essential for exposing pertinent features of the data. In general, the coupled-channels theory, when using appropriate ion-ion potentials, is able to describe the fusion cross section for moderately heavy systems down to an energy just below the interaction barrier. Recently, it was found that to reproduce fusion cross sections at above barrier energies it was necessary to increase the diffuseness parameter to values larger than those derived from elastic scattering data [8]. This effect is possibly associated with the opening of the deep-inelastic reaction channel. For very heavy systems, it is well known that dynamical effects hinder the formation of a compound nucleus leading to more complicated exit channels such as deep inelastic and quasi-fission processes. The dynamical hindrance of fusion in such systems has been described as a diffusion process which may eventually reach the configuration of the compound nucleus [9].

Recently, a new phenomenon of hindrance in heavy-ion fusion reactions has been found in medium-heavy systems [10, 11, 12, 13]. This hindrance occurs at extreme sub-barrier energies whereas the fusion cross section at near barrier energies agrees fairly well with standard coupled-channels calculations. At present, the exploration of this hindrance phenomenon is only in its initial stage; the underlying physics reason is still unknown. Several colliding systems have been measured down to very low cross section levels. In addition, many existing data have been reanalyzed in order to uncover systematic trends. Thus, it has been found that the nuclear structure of the fusing nuclei plays a decisive role for the onset energy for

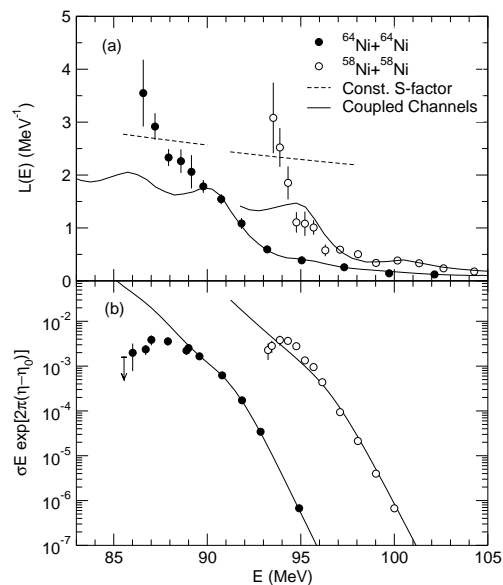


FIG. 1: Comparison of the logarithmic derivative and S -factor representations of the fusion cross section for the systems, $^{58}\text{Ni}+^{58}\text{Ni}$ [14] and $^{64}\text{Ni}+^{64}\text{Ni}$ [12]. The dashed curves correspond to a constant S -factor, whereas the solid curves display results of coupled-channels calculations. The $L(E)$ data were obtained from a fit to the cross sections at three consecutive beam energies.

the hindrance in medium-heavy systems [12, 13]. In the present paper, we study the dependence of the hindrance on the mass, and by extension also on the Q -value of the fusing systems over a wide range of projectile-target combinations. In general, the Q -value becomes less negative with decreasing mass, and even positive for the lightest systems. We note that the possible occurrence of fusion hindrance in the lightest nuclei is of great astrophysical interest.

In order to be able to recognize the hindrance in the rapidly varying sub-barrier fusion cross sections, we have earlier studied the effect in terms of two representations, which are not often used in heavy-ion fusion studies. These are the logarithmic derivative, $L(E) = d\ln(\sigma E)/dE$ and the S -factor, $S(E) = \sigma E \exp(2\pi\eta)$, where $\eta = Z_1 Z_2 e^2 / (\hbar v)$ is the Sommerfeld parameter

[10, 11, 12, 13]. In Fig. 1 these quantities are given for the $^{58}\text{Ni}+^{58}\text{Ni}$ and $^{64}\text{Ni}+^{64}\text{Ni}$ systems. The maximum in the S -factor occurs at the energy, E_s , where the logarithmic derivative $L(E)$ crosses the curve for a constant S -factor, which is given by [11]

$$L_{cs}(E) = \pi\eta/E = 0.495Z_1Z_2\sqrt{\mu}/E^{3/2} \quad (\text{MeV}^{-1}), \quad (1)$$

where $\mu = A_1A_2/(A_1+A_2)$ (dashed curves in Fig. 1). We note that the logarithmic slope of the data, $L(E)$, intersects $L_{cs}(E)$ at a substantially larger angle, and therefore the peak in the S -factor is narrower, for $^{58}\text{Ni}+^{58}\text{Ni}$ than for $^{64}\text{Ni}+^{64}\text{Ni}$. This is a consequence of the "stiffness" of the former system. A dependence on the "stiffness" of the fusing nuclei has been seen in many cases such as $^{90}\text{Zr}+^{90,92}\text{Zr}$, ^{89}Y (see Table I column 5) and as discussed in Ref. [10, 11].

A negative fusion Q -value requires that there be a maximum of $S(E)$ [11]. This is a consequence of the fact that the cross section must vanish at a finite center-of-mass energy corresponding to the ground state of the fused system, *i.e.*, at $E = -Q$. In this limit, $L(E) = \sigma^{-1}d\sigma/dE + 1/E \rightarrow +\infty$, whereas $L_{cs}(E)$ remains finite. This means that for such systems there is always an energy for which the S -factor has a maximum. This occurs when $L(E)$ becomes equal to $\pi\eta/E$, a condition that is always fulfilled, since $\pi\eta/E$ is finite near and above $E = -Q$, whereas $L(E) = d\ln(\sigma E)/dE$ approaches infinity as $E \rightarrow -Q$.

For positive Q -value systems, however, a maximum may not develop, because both $L(E)$ and $L_{cs}(E)$ become infinite in the limit of $E = 0$. If $L(E)$ does not grow faster than $L_{cs}(E)$ with decreasing energy, it may not cross $L_{cs}(E)$ for any positive value of E . It is, therefore, of interest to study the systematics of the sub-barrier fusion hindrance over a wide range of systems, including some with positive Q -value, as is the case mainly in fusion between lighter nuclei.

The expected dependence on the Q -value of the system appears to be borne out by data. The systematics of the logarithmic derivative $L(E)$ of fusion excitation functions is illustrated in Fig. 2 for a number of systems ranging from $^{10}\text{B}+^{10}\text{B}$ to $^{90}\text{Zr}+^{92}\text{Zr}$. The logarithmic derivatives are represented by open circles for five-point derivatives, whereas the open squares were obtained by a fit to three consecutive data points. We observe that $L(E)$ for all systems increases with decreasing energy. The dashed curves represent the logarithmic slopes corresponding to a constant S -factor (Eq. 1). In an earlier study of fusion between "stiff" nuclei [11], which did not include systems lighter than $^{16}\text{O}+^{144}\text{Sm}$, we found that the S -factor maximum systematically occurred at a value of $L_s = 2.33 \text{ MeV}^{-1}$ corresponding to

$$E_s^{ref} = 0.356 (Z_1Z_2\sqrt{\mu})^{2/3} \quad (\text{MeV}). \quad (2)$$

Studying the full range of systems, we observe that the crossing point, E_s , for lighter systems, which have increasingly positive Q -values, indeed occurs at larger values of $L(E)$. For the lightest systems, the logarithmic

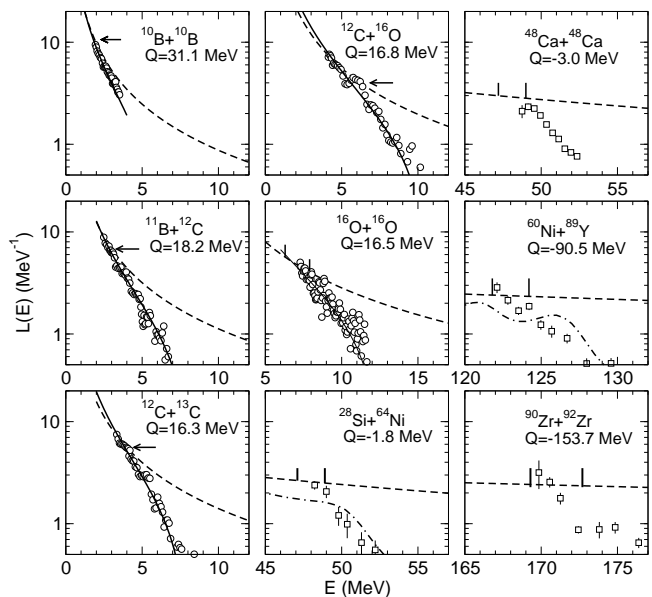


FIG. 2: Logarithmic derivative representations for a range of systems. The dashed curves correspond to a constant S -factor, whereas the dashed-dotted curves display results of coupled-channels calculations, and the solid curves represent a fit to the data using the function $a + b/E^{3/2}$. The range of E_s values are indicated by vertical line segments for heavy systems. For the four lightest systems only lower limits of L_s can be derived (shown as arrows). The data are taken from Refs.: $^{10}\text{B}+^{10}\text{B}$ [15], $^{11}\text{B}+^{12}\text{C}$, $^{12}\text{C}+^{13}\text{C}$, $^{12}\text{C}+^{16}\text{O}$, $^{16}\text{O}+^{16}\text{O}$ [16], $^{48}\text{Ca}+^{48}\text{Ca}$ [17], $^{60}\text{Ni}+^{89}\text{Y}$ [10], and $^{90}\text{Zr}+^{92}\text{Zr}$ [18].

derivatives of the data intersect the constant S -factor curve at a small angle and it is, therefore, difficult to accurately estimate E_s . Consequently, we have used fits to the data with the expression $a + b/E^{3/2}$ (solid curves), a and b being adjustable parameters, to obtain a less subjective estimate of E_s . The results are given in Table I. Relatively large error bars are, however, assigned to the resulting E_s values and, for the lightest systems, only upper limits are given, because of the inaccuracy of this procedure. We also observe that the value of the logarithmic slope, $L(E)$, obtained by coupled-channels calculations for heavy systems (dashed-dotted curves in Fig. 2) saturates at a value of $\sim 1.5 - 2.0 \text{ MeV}^{-1}$, much lower than measured. It has been shown that coupled-channels calculations using reasonable ion-ion potentials are unable to reproduce the extreme sub-barrier behavior [11].

The systematics of sub-barrier hindrance is illustrated in Fig. 3. Here, the derived values of E_s and $L_s = L(E_s)$ are plotted as a function of the parameter $Z_1Z_2\sqrt{\mu}$ in panels a) and b), respectively. Aside from local deviations of L_s from the value of 2.33 MeV^{-1} in medium-heavy systems (of the order of $\sim 10\%$, arising from nuclear structure effects) L_s clearly starts deviating from this value in lighter systems. The corresponding E_s values also fall below the E_s^{ref} systematics (solid curve)

TABLE I: This table lists the parameter $Z_1Z_2\sqrt{\mu}$, the energy E_s and the logarithmic derivative, $L_s = L(E_s)$, that characterize the maximum of the S -factor for different systems. Also given are the $(dL/dE)_{exp}$ and $(dL/dE)_{cs}$, corresponding to the measured and the constant S -factor curves at E_s . R is the ratio $(dL/dE)_{exp}/(dL/dE)_{cs}$, Q is the fusion Q -value, and V_{Bass} is the height of the Bass barrier [19]. Systems in categories I and II exhibit a clear maximum in the $S(E)$ curve for "stiff" and "soft" systems, respectively. A maximum has not quite been reached for systems in category III and IV. Extrapolated values of E_s and L_s etc. are listed for category III, and only upper limits for E_s (lower limits of L_s) are included for most category IV systems. Uncertainties are given in parentheses for E_s , $(dL/dE)_{exp}$ and R . In cases where only upper limits for E_s can be given the values of $(dL/dE)_{exp}$, $(dL/dE)_{cs}$, and R correspond to the crossing points obtained from the fit to the data. Uncertainties for L_s and $(dL/dE)_{cs}$ can be obtained from the uncertainties on E_s with the constant S -factor formula.

System	$Z_1Z_2\sqrt{\mu}$	E_s (MeV)	L_s (MeV ⁻¹)	$(dL/dE)_{exp}$ (MeV ⁻²)	$(dL/dE)_{cs}$ (MeV ⁻²)	R	Q (MeV)	V_{Bass} (MeV)	Ref.
Category I									
⁹⁰ Zr+ ⁹⁰ Zr	10733	175(1.8)	2.29	-1.61(0.16)	-0.020	81.9(8.2)	-157.35	195.3	[18]
⁹⁰ Zr+ ⁸⁹ Y	10436	171(1.7)	2.31	-1.12(0.08)	-0.020	55.1(4.4)	-151.53	190.1	[18]
⁹⁰ Zr+ ⁹² Zr	10792	171(1.7)	2.40	-0.84(0.07)	-0.021	39.0(3.6)	-153.71	184.4	[18]
⁵⁸ Ni+ ⁵⁸ Ni	4222	94(0.9)	2.29	-1.64(0.31)	-0.036	44.9(8.6)	-66.122	102.0	[14]
⁶⁰ Ni+ ⁸⁹ Y	6537	123(1.2)	2.38	-0.80(0.19)	-0.029	27.5(6.6)	-90.497	136.5	[10]
³² S+ ⁸⁹ Y	3026	72.6(0.7)	2.42	-0.58(0.15)	-0.050	11.5(3.0)	-36.597	79.8	[20]
Category II									
⁶⁴ Ni+ ¹⁰⁰ Mo	7343	121(1.2)	2.74	-0.57(0.09)	-0.034	17.0(2.7)	-92.287	143.3	[13]
⁶⁴ Ni+ ⁶⁴ Ni	4435	87.3(0.9)	2.69	-0.35(0.02)	-0.046	7.7(0.5)	-48.783	98.1	[12]
Category III									
⁴⁸ Ca+ ⁴⁸ Ca	1960	48.1(0.9)	2.90	-0.59(0.03)	-0.090	6.5(0.5)	-2.988	50.1	[17]
²⁸ Si+ ⁶⁴ Ni	1729	47.3(0.9)	2.57	-0.70(0.12)	-0.080	8.7(1.7)	-1.783	50.8	[21]
¹⁶ O+ ⁷⁶ Ge	930.5	27.6(0.8)	3.17	-0.36(0.05)	-0.172	2.1(0.2)	10.506	32.5	[22]
Category IV									
¹⁶ O+ ¹⁶ O	181.0	7.1(0.8)	4.7(0.7)	-1.7(0.2)	-1.0	1.7(0.2)	16.542	8.2	[16, 23, 24, 25, 26]
¹² C+ ¹⁶ O	125.7	<6.2	>4.0	-3.0	-2.2	1.4	16.756	6.0	[16, 27, 28, 29]
¹² C+ ¹⁴ N	106.8	<5.0	>4.7	-4.1	-3.2	1.3	15.074	5.2	[16]
¹² C+ ¹³ C	89.9	<4.0	>5.6	-3.9	-2.7	1.4	16.318	4.3	[16]
¹¹ B+ ¹² C	71.9	<3.0	>6.8	-8.8	-7.6	1.2	18.198	3.5	[16]
¹⁰ B+ ¹⁰ B	55.9	<1.9	>10.6	-26.6	-24.4	1.1	31.144	2.9	[15]

given in Eq. 2. A purely empirical expression

$$L_s^{emp} = 2.33 + 400/(Z_1Z_2\sqrt{\mu}) \quad (\text{MeV}^{-1}) \quad (3)$$

(dashed curve in Fig. 3b) is seen to provide a good approximation to the experimental data, and it reproduces the asymptotic value of 2.33 MeV⁻¹ observed earlier for heavy systems with $Z_1Z_2\sqrt{\mu} > 2500$. The corresponding curve for E_s^{emp} obtained from Eqs. 1 and 3, namely

$$E_s^{emp} = (0.495Z_1Z_2\sqrt{\mu}/L_s^{emp})^{2/3} \quad (\text{MeV}), \quad (4)$$

is seen also to reproduce the experimental values in Fig. 3a. These two equations thus represent the overall systematics for the onset of sub-barrier fusion hindrance. This systematics appears to be correlated with the parameter $Z_1Z_2\sqrt{\mu}$ in the simple fashion expressed in Eqs. 3 and 4, but it should be kept in mind that both the Q -value and the fusion (interaction) barrier vary smoothly, although not quite monotonically, with this parameter. Hence, it is not possible to ascertain whether the observed physical effect of fusion hindrance is associated with either, or with both of these quantities.

Figure 3c presents the ratio of the logarithmic slopes, $R = (dL/dE)_{exp}/(dL/dE)_{cs}$, for the data relative to the

constant S -factor curve. For $Z_1Z_2\sqrt{\mu} > 2000$, this ratio is substantially larger than unity which means that there is a sharp intersection point between the two curves and, consequently, a well defined, narrow maximum in the S -factor curve. For $Z_1Z_2\sqrt{\mu}$ values below about 2000, the slope ratio approaches unity which results in a less well defined intercept point. For the lightest systems, it appears that the logarithmic slope of the data approaches the value for a constant S -factor and the sub-barrier hindrance may well disappear.

It should be emphasized that $L_{cs}(E)$ equals the logarithmic derivative in a point charge, pure Coulomb penetration model, as long as η is greater than ~ 10 , which is always the case in the energy range studied here. A relative slope, $R \gg 1$, therefore, implies that the fusion cross section drops more rapidly than predicted in a point charge pure Coulomb interaction model, whereas a relative slope near unity indicates that the fusion cross section decreases at the predicted rate.

For orientation, it may also be of interest to relate the observed values of E_s to the fusion (or interaction) barrier and the Q -value of the fusion process, as given in Fig. 3d and 3e as a function of the parameter $Z_1Z_2\sqrt{\mu}$. Since the cross section must vanish at an energy of $E = -Q$ (for

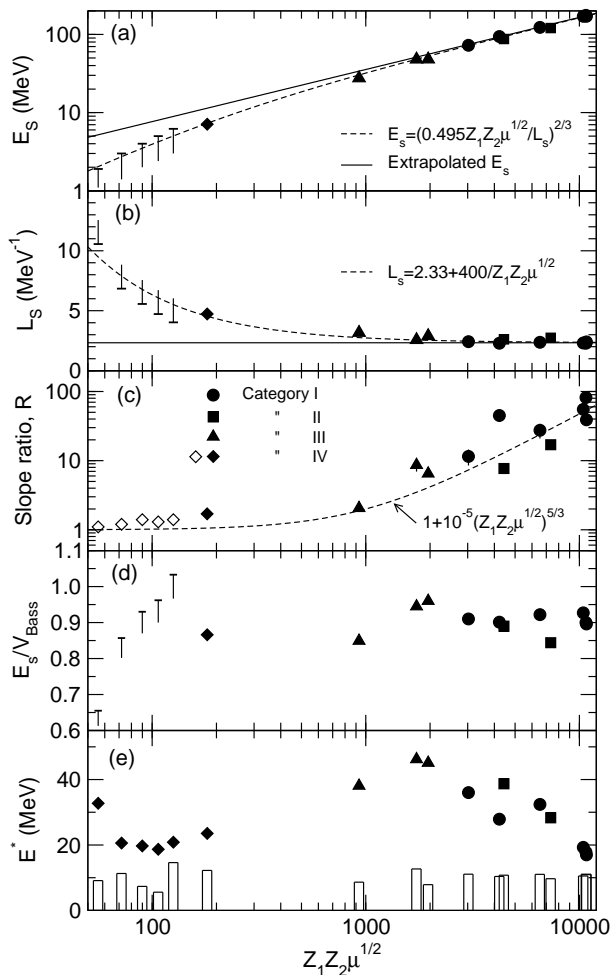


FIG. 3: (a) Experimental values (symbols) and limits (horizontal bars) are shown as a function of $Z_1 Z_2 \sqrt{\mu}$ for E_s (panel a), L_s (panel b), logarithmic slope ratio, $R = (dL/dE)_{exp}/(dL/dE)_{cs}$ at E_s (panel c), ratio E_s/V_{Bass} (panel d), and $E^* = E_s + Q$ (panel e), which also shows effective particle emission thresholds (histogram). Solid lines in panels a) and b) correspond to $L_s = 2.33 \text{ MeV}^{-1}$, whereas dashed curves represent empirical trends of the data. Open diamonds in panel c) represents the slope ratio at the crossing point obtained from the fit to the data.

$Q < 0$) or $E = 0$ (for $Q > 0$), the larger of these two values represents a lower bound for E_s . On the other hand, one may consider the fusion barrier, taken here from the Bass prescription [19], V_{Bass} , as an upper bound for E_s . In Fig. 3d, the experimental values of E_s do not appear to have a simple or fixed relation to V_{Bass} : the onset of sub-barrier hindrance, E_s , occurs at an energy between 5% and 35% below the fusion barrier. Furthermore, relatively large fluctuations between systems with similar values of the parameter $Z_1 Z_2 \sqrt{\mu}$ are present, some of which are clearly related to the structure of the fusing nuclei [12, 13].

A potential cause of fusion hindrance at sub-barrier energies could be the rarefication of final states accessible

in the fused system, which may be expressed as the ratio of total width to the spacing of the states, *i.e.* Γ^{tot}/D , in the appropriate energy regime of the compound nucleus. In other words, a fusion reaction can only proceed if a quantum state with the appropriate energy, spin and parity is available in the compound nucleus. The Γ^{tot}/D value is expected to increase exponentially with excitation energy and will approach unity slightly above the particle (n, p, or α) emission threshold (binding energy + Coulomb barrier). In order to explore this possibility, we have plotted in Fig. 3e, the excitation energy corresponding to E_s , *i.e.*, $E_s + Q$ (solid symbols) and compared it to the particle thresholds for the systems listed in Table I. We note that the experimental values of E_s correspond to excitation energies exceeding the particle thresholds by a wide margin in all cases, and there does not appear to be a significant correlation between these two quantities. Even accounting for the fact that some of the excitation energy is bound in rotational energy does not alter this conclusion. Although the simple explanation of rarefication of the final states in the fusion process is appealing, it does not appear to account for the observed hindrance phenomenon. It seems that the behavior seen in Fig. 3a-c provides indications that the hindrance phenomenon is closely related to the entrance channel.

In conclusion, the systematics of sub-barrier fusion hindrance has been studied over a wide range of systems from $^{10}\text{B}+^{10}\text{B}$ to $^{90}\text{Zr}+^{90}\text{Zr}$. Hindrance appears to be a general phenomenon, at least for systems with $Z_1 Z_2 \sqrt{\mu} \gtrsim 3000$. For the lightest systems ($Z_1 Z_2 \sqrt{\mu} \lesssim 200$), the logarithmic slopes of the cross section in the sub-barrier region merge smoothly into those expected on the basis of a constant S -factor (*i.e.* a point charge in a pure Coulomb interaction model). Simple empirical formulae are given for both the energy and the logarithmic slope of the cross section at which the onset of fusion hindrance occurs. These point to an entrance channel effect as the source of this phenomenon. Until now, all direct observations of fusion hindrance have been made in systems with $Z_1 Z_2 \sqrt{\mu} \gtrsim 3000$. It would be interesting to study sub-barrier fusion in more systems in the range $200 \lesssim Z_1 Z_2 \sqrt{\mu} \lesssim 3000$, where the fusion Q -values change from positive to negative values. If the fusion hindrance does indeed occur in light systems, such as $^{12}\text{C}+^{12}\text{C}$, $^{12}\text{C}+^{16}\text{O}$ and $^{16}\text{O}+^{16}\text{O}$, it will strongly affect the predicted rates of astrophysical processes, which are presently obtained by simple empirical extrapolations from experimental data. As yet, no satisfactory theoretical explanation for this phenomenon has been put forth. Simple considerations in terms of relations to the fusion barrier height or the rarefication of compound states in the fusion channel do not appear to clarify the situation.

This work was supported by the U.S. Department of Energy, Office of Nuclear Physics, under contract No. W-31-109-ENG-38.

-
- [1] M. Beckerman, Physics Report, **129**, 145 (1985).
[2] M. Beckerman, Rep. Prog. Phys. **51**, 1047 (1988).
[3] K. Hagino, N. Takigawa, M. Dasgupta, D. J. Hinde and J.R. Leigh, Phys. Rev. C **55**, 276 (1997).
[4] A. B. Balantekin and N. Takigawa, Rev. Mod. Phys. **70**, 77 (1998).
[5] R. Vandenbosch, Annu. Rev. Nuc. Part. Sci. **42**, 447 (1992).
[6] N. Rowley, G. R. Satchler and P.H.Stelson, Phys. Lett. **B254**, 25 (1991).
[7] M. Dasgupta, D.J. Hinde, N. Rowley and A.M. Stefanini, Annu. Rev. Nucl. Part. Sci. **48**, 401 (1998).
[8] J. O. Newton *et al.*, Phys. Lett. **B 586**, 219 (2004); Phys. Rev. C **70**, 024605 (2004).
[9] W. J. Swiatecki, A. Trzcinska, and J. Jastrzebski, Phys. Rev. C **71**, 047301 (2005).
[10] C.L. Jiang *et al.*, Phys. Rev. Lett. **89**, 052701 (2002).
[11] C.L. Jiang, H.Esbensen, B.B. Back, R.V.F. Janssens and K.E. Rehm, Phys. Rev. C. **69**, 014604 (2004).
[12] C.L. Jiang *et al.*, Phys. Rev. Lett. **93**, 012701 (2004).
[13] C.L. Jiang *et al.*, Phys. Rev. C **71**, 044613 (2005).
[14] M. Beckerman *et al.*, Phys. Rev. C **23**, 1581 (1982).
[15] M.D. High and B. Cujec, Nucl. Phys. **A259**, 513 (1976).
[16] R.G. Stokstad *et al.*, Phys. Rev. Lett. **37** 888 (1976).
[17] M. Trotta *et al.*, Phys. Rev. C **65**, 011601 (2002).
[18] J. G. Keller *et al.*, Nucl. Phys. **A452**, 173 (1986). Phys. Lett. B **254**, 25 (1991).
[19] R.Bass, Nucl. Phys. **A231**, 45 (1974).
[20] A. Mukherjee, *et al.*, Phys. Rev. C **66**, 034607 (2002).
[21] A.M. Stefanini *et al.*, Nucl. Phys. **A456**, 509 (1986).
[22] E.F. Aguilera, J.J. Kolata and R.J. Tighe, Phys. Rev. C **52**, 3103 (1995).
[23] H. Spinka *et al.*, Nucl. Phys. **A233** 456 (1974).
[24] S.C. Wu and C.A. Barnes, Nucl. Phys. **A422**, 373 (1984).
[25] J. Thomas *et al.*, Phys. Rev. C **31**, 1980 (1985).
[26] G. Hulke *et al.*, Z. Phys. **A297**, 161 (1980).
[27] B. Cujec *et al.*, Nucl. Phys. **A266** 461 (1976).
[28] Z.E. Switkowski *et al.*, Nucl. Phys. **A274** 202 (1976).
[29] J.R. Patterson, H. Winkler and C. S. Zaidins, Astrophys. J. **157**, 367 (1969).